Ninth International Conference on Computational Fluid Dynamics (ICCFD9), Istanbul, Turkey, July 11-15, 2016

ICCFD9-2016-226

Parametric Investigation of Hull Shaped Fuselage for an Amphibious UAV

Emre Sazak[1], D. Funda Kurtulus[2]

[1] M.Sc. Student, Department of Aerospace Engineering, Middle East Technical University, Ankara 06800, Turkey

[2] Assoc. Prof., Department of Aerospace Engineering, Middle East Technical University, Ankara 06800, Turkey

Corresponding author: emre.sazak@metu.edu.tr

Abstract: Performance of amphibious UAV's (Unmanned Aerial Vehicles) that take off from and land on water, like seaplanes, greatly depend on hydrodynamic effects as well as aerodynamic effects, therefore their geometries need to be optimized. This study mainly investigates the effect of geometric parameters of a generic, hull-shaped fuselage that are constrained by hydrodynamic drivers, such as the step height needed to reduce hydrodynamic drag, and deadrise and sternpost angles needed for safe landing, on aerodynamic drag of the fuselage under cruise conditions by means of the commercial CFD code ANSYS Fluent. Study includes a comparison of the experimental [1] and numerical results obtained at angles of attack varying between 8° to 16° and with Spalart-Allmaras, k-ω and k-ε turbulence models.

Keywords: Amphibious UAV, Computational Fluid Dynamics, Turbulence Modeling.

1 Introduction

An amphibious aircraft is defined as an aircraft that can take off from and land on water, with most popular of these kinds of aircraft being seaplanes. While widely used from the start of modern aviation, seaplane usage deteriorated rapidly after the end of WWII due to wide availability and increasing length of runways, since seaplanes were aerodynamically inferior compared to conventional aircraft and there were little need to compensate for the increased fuel consumption and lower speed and range; and military usage has further diminished with the introduction and widespread usage of radars, helicopters and aircraft carriers. Nowadays mostly used for travelling to remote locations with water, firefighting, sports, oceanographic studies and search & rescue missions, recent progress in UAV's shows potential for amphibians to be widely used again in the future [2, 3].

Amphibians can be divided into two categories depending on their shape of fuselages, floatplanes and flying boats. Floatplanes have floats (also called sponsons or pontoons) mounted under their fuselage that provide buoyancy, while flying boats have fuselages designed as a ship's hull for the purpose of granting buoyancy and moving through water. Many amphibious aircraft have flying boat type fuselages, which is also well suited for unmanned operations due to their tendency of having lower drag, better stability on water and lower empty weight compared to floatplanes and lack of need for boarding the aircraft on water [4].

Flying boat fuselages and floatplane floats have been very similar in shape, and other than the step and the sternpost angle, similar with high-speed planing boats such as speedboats; and they possess the same geometric entities at the lower half of their structures due to being exposed to same hydrodynamic and aerodynamic effects. Various models of both have been extensively studied by NACA (National Advisory Committee for Aeronautics) by means of towing tank and wind tunnel experiments, for the purposes of determining hydrodynamic and aerodynamic characteristics, respectively, and reducing aerodynamic drag without affecting hydrodynamic performance.

2 Problem Statement

Amphibious aircrafts operate both on water and air, therefore their performance is highly dependent on the optimization of their shape. Shape of the fuselage is constrained primarily by hydrodynamic performance requirements needed for safe take-off and landing, which in turn affects the aerodynamic performance of the aircraft, especially at cruise condition.

Geometric parameters of a generic amphibious aircraft fuselage are shown on front and side views of the CAD model of NACA Model 57-A Hull in Figures 1 and 2:

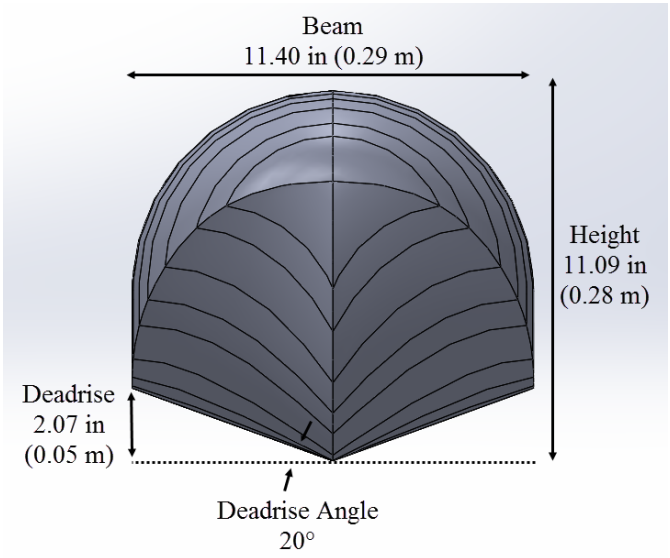

Figure 1: Geometric parameters shown on front view of NACA 57-A Hull CAD model

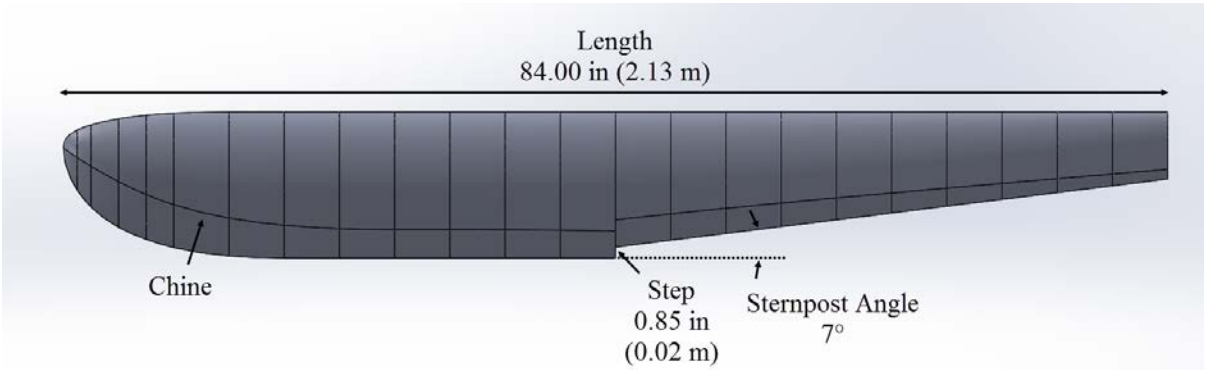

Figure 2: Geometric parameters shown on side view of NACA 57-A Hull CAD model

Step is the vertical discontinuity located at the bottom of the hull required to break contact with water and overcome hydrodynamic drag occurring due to vacuum of the water during take-off, while deadrise angle is the upward angle from horizontal of the hull bottom that is needed to reduce water impact loads and sternpost angle is the angle that the rear section of the fuselage makes with the horizontal, needed to avoid contact with the water during take-off [5, 6].

Typical ranges of parameters are given in Table 1:

Table 1: Range of fuselage geometric parameters

Fuselage Parameter	Range
Step Height	4% to 8% of beam [7]
Deadrise Angle	15° to 40° [5]
Sternpost Angle	7° to 9° [5]

To investigate the effects of geometric parameters of a hull-shaped fuselage on aerodynamic drag of the body, CFD analyses have been conducted on a CAD model of a generic hull shape (NACA Model 57-A) described in NACA Technical Note No. 716. The models were created by extrapolating available data of cross-sectional dimensions [1].

3 Numerical Method

3.1 Governing Equations

The Reynolds-Averaged Navier-Stokes (RANS) equations used to define fluid motion in turbulent flows, with mean and fluctuating flow quantities represented in Einstein notation are given in equations (1) and (2):

$$\frac{\partial \rho}{\partial t} + \frac{\partial}{\partial x_i}(\rho u_i) = 0 \tag{1}$$

$$\frac{\partial}{\partial t}(\rho u_i) + \frac{\partial}{\partial x_j}(\rho u_i u_j) = -\frac{\partial p}{\partial x_i} + \frac{\partial}{\partial x_j}\left[\mu\left(\frac{\partial u_i}{\partial x_j} + \frac{\partial u_j}{\partial x_i} - \frac{2}{3}\delta_{ij}\frac{\partial u_l}{\partial x_l}\right)\right] + \frac{\partial}{\partial x_j}\left(-\rho\overline{u_i' u_j'}\right) \tag{2}$$

Here, flow quantities are decomposed to mean and fluctuating components, such that:

$$u_i = \overline{u}_i + u_i' \tag{3}$$

for velocity and

$$\phi = \overline{\phi} + \phi' \tag{4}$$

for scalar quantities. Here, the non-linear Reynolds stress term $\left(-\rho\overline{u_i' u_j'}\right)$ in equation (2) needs to be modeled in order to overcome the closure problem arising from the lack of equations needed to solve for the unknowns. Together by applying the Boussinesq approximation,

$$-\rho\overline{u_i' u_j'} = \mu_t\left(\frac{\partial u_i}{\partial x_j} + \frac{\partial u_j}{\partial x_i}\right) - \frac{2}{3}\left(\rho k + \mu_t\frac{\partial u_k}{\partial x_k}\right)\delta_{ij} \tag{5}$$

where μ_t is the turbulent viscosity considered as a flow property; Reynolds stress term is modeled using one-equation and two-equation turbulence models [8, 9, 10].

3.2 Application

Drag coefficient is defined with the following relation:

$$C_D = \frac{D}{q(vol)^{2/3}} \tag{6}$$

Where C_D is the drag coefficient, D is the drag force, q is the dynamic pressure and vol is the volume of the body. Here, volume is used instead of the area due to being an independent design variable [1].

Measured values of drag coefficient given in NACA Technical Note No. 716 was compared to numerical results obtained from commercial CFD code ANSYS Fluent 3D RANS solver under steady-state, incompressible flow assumptions; and by using Spalart-Allmaras, SST k-ω and Realizable k-ε turbulence models, which have been widely applied for analyses of a wide range of flows. Aerodynamic tests described in NACA Technical Note No. 716 were conducted in NACA Langley 7-by-10-foot Wind Tunnel, which had an open-jet test chamber with a cross-section of 2.13 x 3.05 m [1, 11].

Velocity Inlet with a magnitude of 35.78 m/s (80.04 mph), Pressure Outlet corresponding to atmospheric pressure, Symmetry and No-slip Wall boundary conditions were applied to relevant boundaries of computational domain to obtain the experimental dynamic pressure of 262.22 kg/m^3 (16.37 lb/ft^3) with the air density of 1.225 kg/m^3, which results in a flow Reynolds Number of 5.2x10^6 and a Mach Number of 0.1.

It was seen that the case with SST k-ω turbulence model agreed best with the experimental results, and has been implemented in further analyses. A mesh refinement study has been performed, in which the non-dimensional wall distance on fuselage surface was held constant as $y+_{max} \approx 1$ to resolve the boundary layer to the viscous sublayer, and 8.12 million cell unstructured mesh has proved adequate accuracy without exorbitant CPU time.

View of the mesh from symmetry plane has been shown on Figure 3, and drag coefficient results of mesh refinement study and comparison of various turbulence models have been given in Tables 2 and 3.

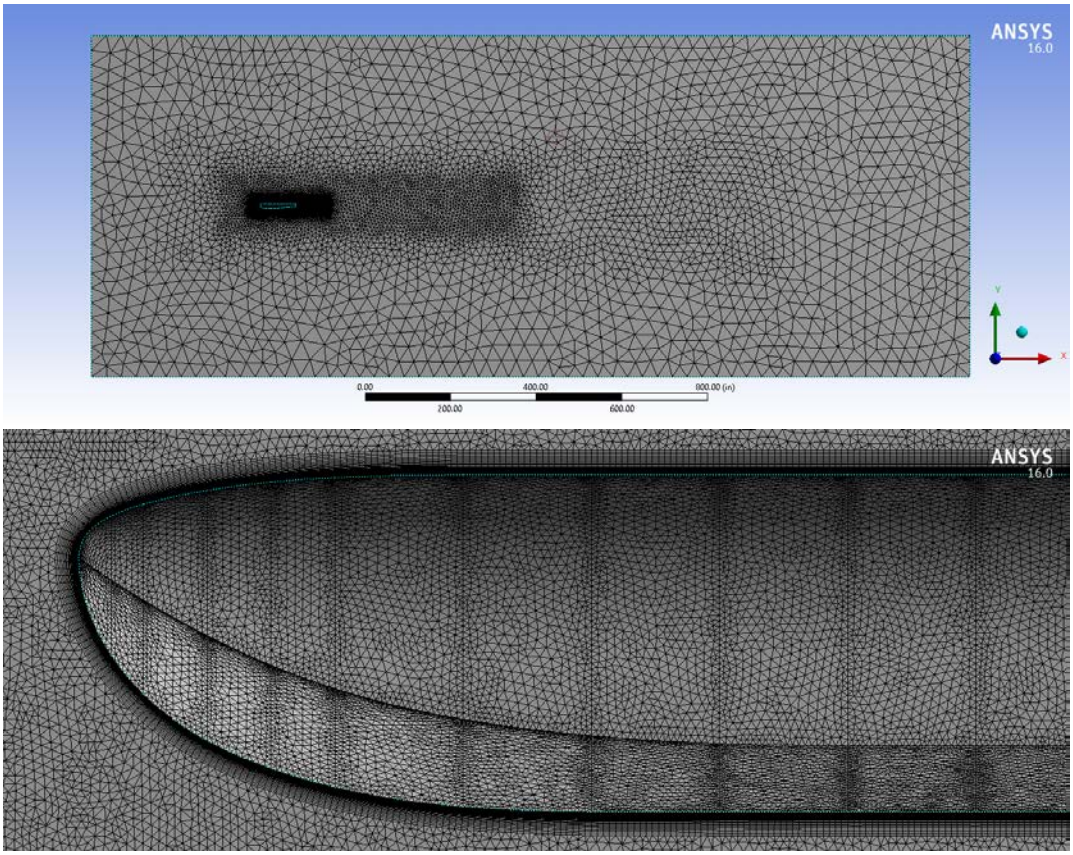

Figure 3: View of computational domain and mesh from symmetry plane

Table 2: Results of drag coefficient for varying mesh resolutions

Mesh Resolution (Million Elements)	C_D
Coarser (2.74)	0.04830
Coarse (4.54)	0.04667
Medium (6.33)	0.04591
Fine (8.12)	0.04523
Finer (9.85)	0.04499
Experimental (NACA-TN-716)	0.04101

Table 3: Comparison of experimental and numerical drag coefficient results obtained at 0° angle of attack using 8.12 million element mesh with various turbulence models

Turbulence Model	C_D
Spalart-Allmaras	0.05025
Realizable k-ε	0.06510
SST k-ω	0.04523
Experimental (NACA-TN-716)	0.04101

Comparison of the experimental and numerical drag coefficient values of base model at various angles of attack, and the pressure coefficient plot of base model on fuselage symmetry plane are given in Figures 4 and 5, respectively.

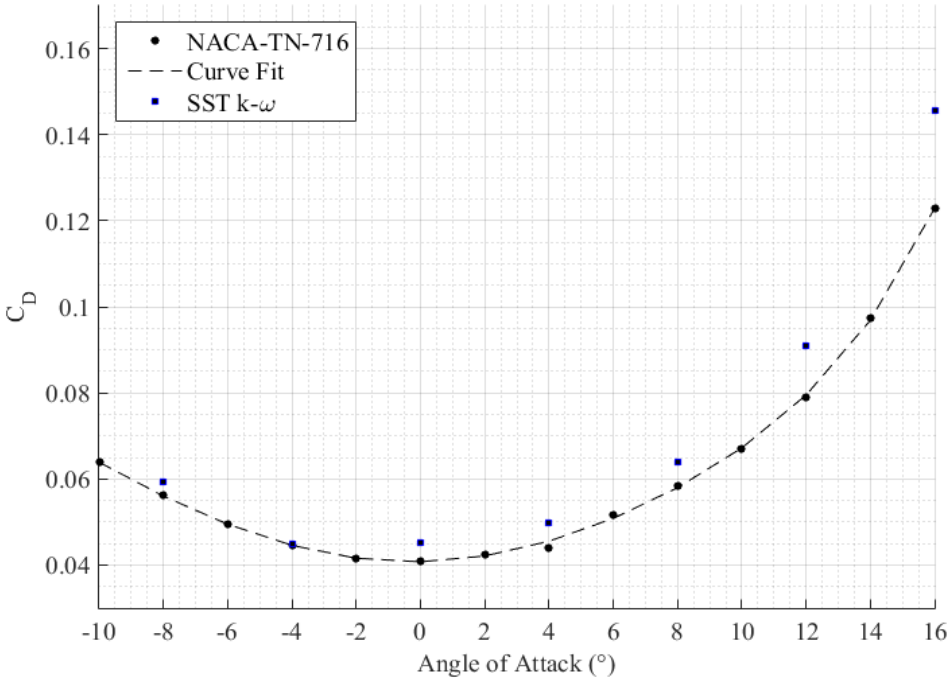

Figure 4: Drag coefficient values of experimental and numerical results of NACA Model 57-A hull under various angles of attack

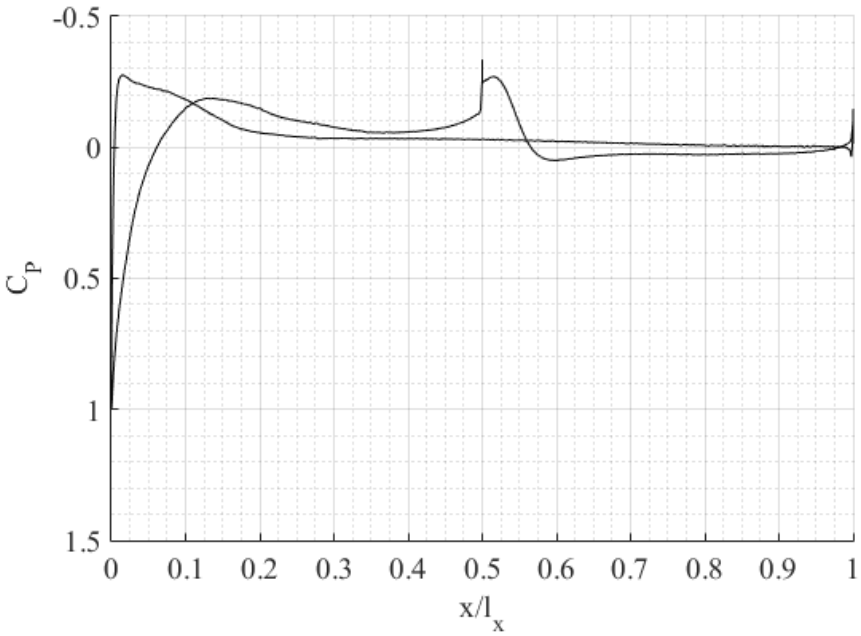

Figure 5: Pressure coefficient plot of the base model

Static pressure and streamwise velocity contours on symmetry plane at 0° angle of attack are given in Figures 6 and 7, and change in velocity contours with varying angles of attack is given in Figure 8:

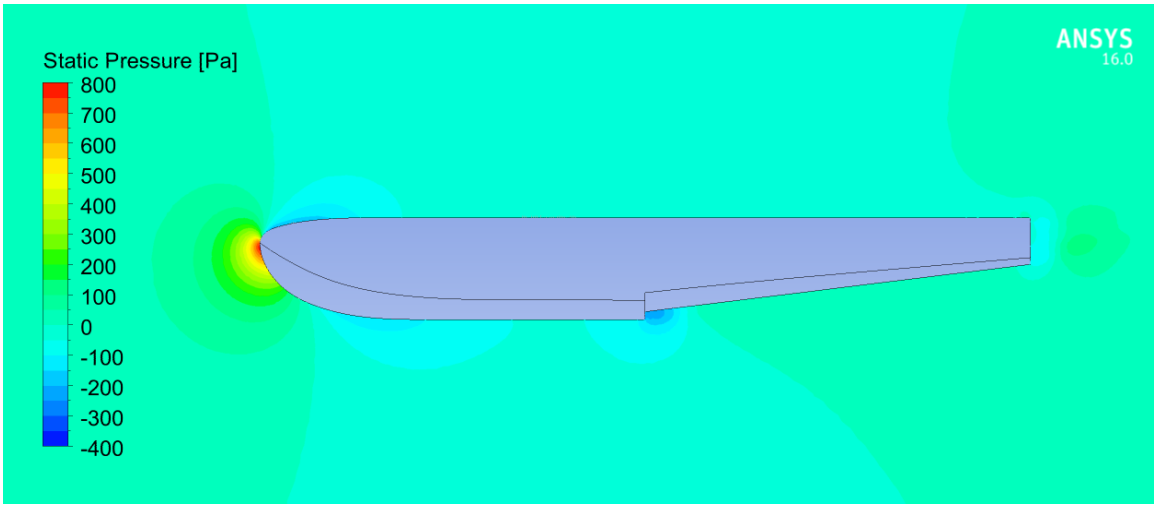

Figure 6: Static pressure contours on symmetry plane of NACA Model 57-A hull at 0° angle of attack

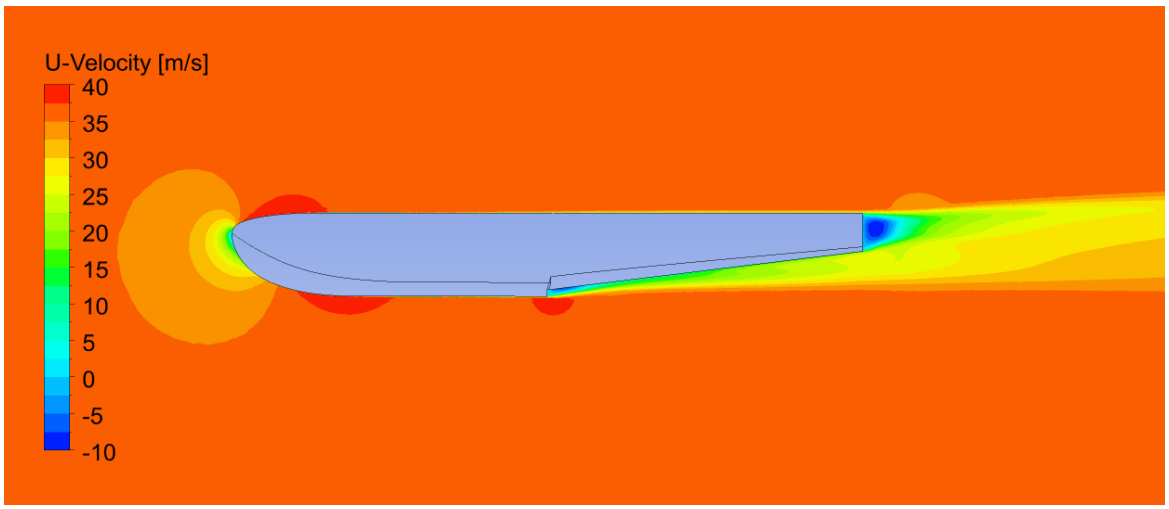

Figure 7: Streamwise velocity contours on symmetry plane of NACA Model 57-A hull at 0° angle of attack

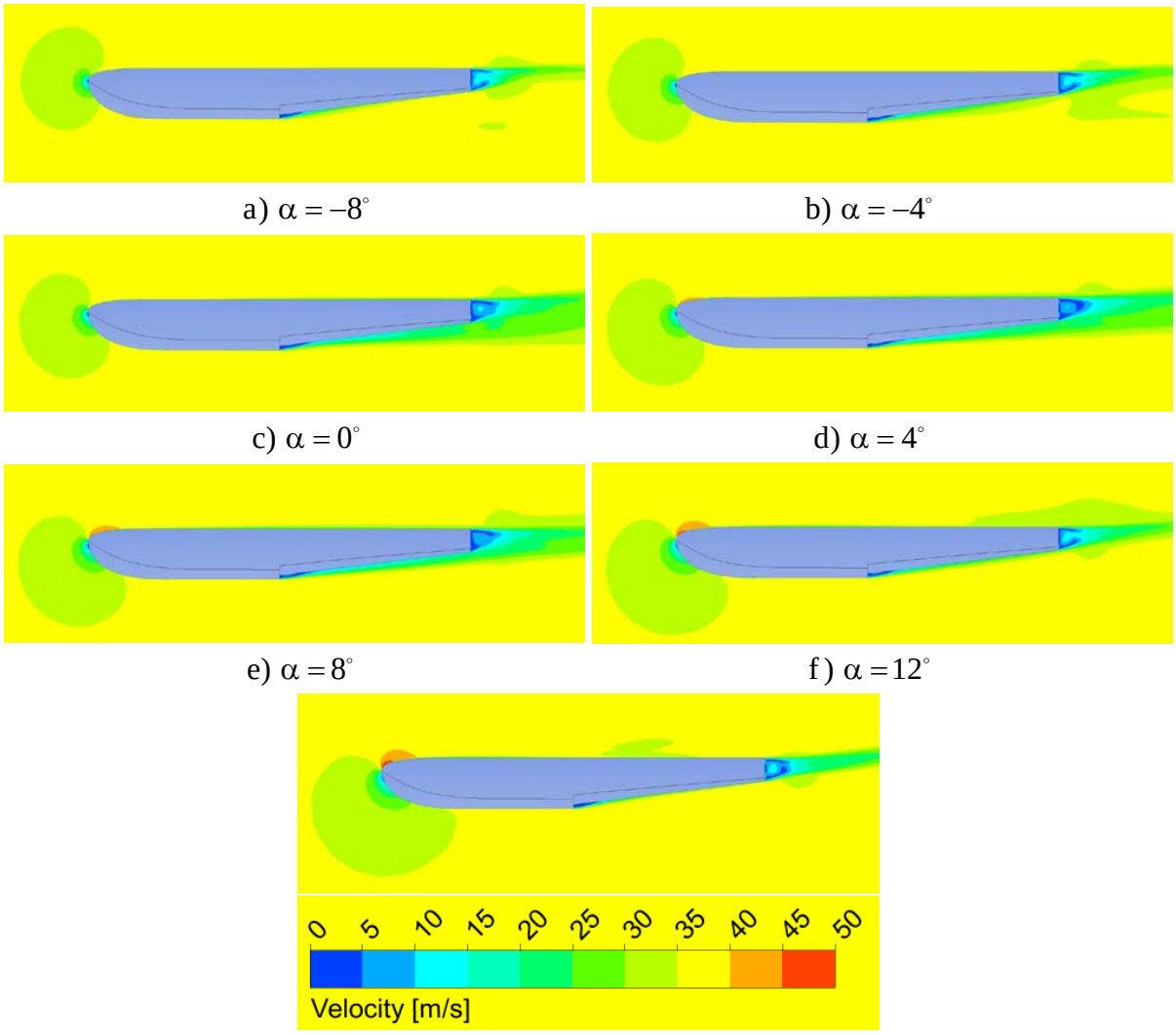

a) $\alpha = -8^{\circ}$ b) $\alpha = -4^{\circ}$

c) $\alpha = 0^{\circ}$ d) $\alpha = 4^{\circ}$

e) $\alpha = 8^{\circ}$ f) $\alpha = 12^{\circ}$

g) $\alpha = 16^{\circ}$

Figure 8: Velocity magnitude contours on symmetry plane of NACA Model 57-A hull at various angles of attack

Streamlines are shown on symmetry plane in Figure 9:

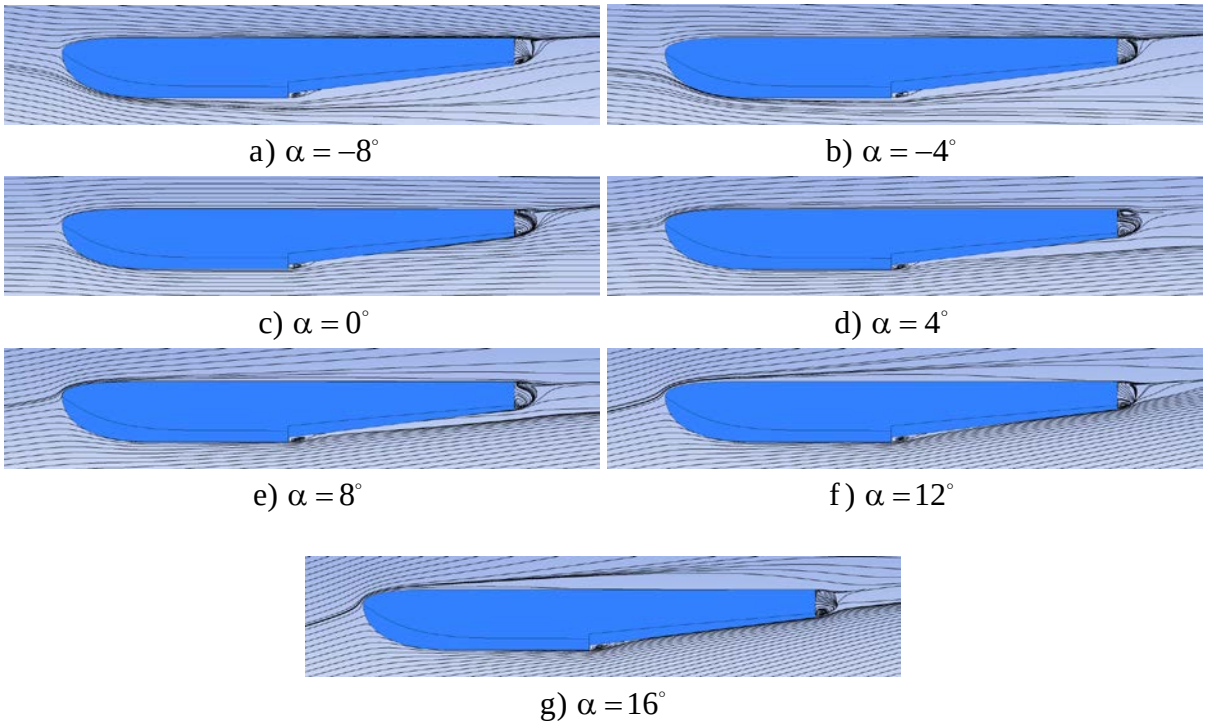

a) $\alpha = -8^{\circ}$ b) $\alpha = -4^{\circ}$

c) $\alpha = 0^{\circ}$ d) $\alpha = 4^{\circ}$

e) $\alpha = 8^{\circ}$ f) $\alpha = 12^{\circ}$

g) $\alpha = 16^{\circ}$

Figure 9: Streamlines on symmetry plane of NACA Model 57-A hull at various angles of attack

Values of drag coefficient obtained using SST k-ω turbulence model for varying step heights, sternpost angles and deadrise angles are given in Tables 4, 5 and 6, respectively.

Table 4: Drag coefficient results of varying step heights

Step Height	C_D	Difference %
0.850 in (0.075 x beam)	0.04523	
0.741 in (0.065 x beam)	0.04433	-2.01
0.627 in (0.055 x beam)	0.04345	-3.95
0.513 in (0.045 x beam)	0.04307	-4.79

Table 5: Drag coefficient results of varying sternpost angles

Sternpost Angle	C_D	Difference %
7°	0.04523	
8°	0.04531	0.16
9°	0.04571	1.06

Table 6: Drag coefficient results of varying deadrise angles

Deadrise Angle	C_D	Difference %
20°	0.04523	
25°	0.04629	2.32
30°	0.04817	6.48

4 Conclusion

Effects of several geometric parameters on aerodynamic drag of the fuselage, along with the comparison of numerical and experimental data were evaluated at the study. The difference between the numerical and experimental results were, to some extent due to computational models of the fuselages being generated by the extrapolation of available cross-sectional dimensions, hence slightly differing in shape from the models in respective studies. The flow is strongly influenced by separation

and eddies at the wake and the step regions (Figures 6, 7, 8, 9), and results obtained with SST k-ω turbulence model, which is widely used for problems with such flows agrees well with the experimental data. Table 4 shows that within hydrodynamic performance constraints, reducing step height results in a decrease in cruise drag as much as 4.79%. While change in sternpost angle from 7° to 8° does not affect drag coefficient significantly, the change in this parameter from 8° to 9° results in an increase of 1.06%, given in Table 5. Table 6 shows that an increase in deadrise angle from 20° to 30° also increases drag coefficient by 6.48%, which makes this parameter relatively having the greatest effect on the drag of the fuselage.

References

[1] J. B. Parkinson, R. E. Olson, and R. O. House. “NACA Technical Note No: 716, Hydrodynamic and Aerodynamic Tests of a Family of Models of Seaplane Floats with Varying Angles of Dead Rise”. NACA. 1939.

[2] A. L. Canamar Leyva. “Seaplane Conceptual Design and Sizing”. University of Glasgow. 2012.

[3] R. D. Eubank. “Autonomous Flight, Fault, and Energy Management of the Flying Fish Solar-Powered Seaplane”. University of Michigan. 2012.

[4] F. I. Petrescu and R. V. Petrescu. *The Aviation History*. Books on Demand. 2012.

[5] S. Gudmundsson. *General Aviation Aircraft Design*. Butterworth-Heinemann. 2013.

[6] D. P. Raymer. *Aircraft Design: A Conceptual Approach, 5th ed.* AIAA. 2012.

[7] D. Stinton. *The Design of the Aeroplane*. BSP Professional Books. 1985.

[8] D. C. Wilcox. “Reassessment of the scale-determining equation for advanced turbulence models". AIAA Journal, Vol. 26, No. 11 (1988), pp. 1299-1310.

[9] P. R. Spalart, S. R. Allmaras. “A One-Equation Turbulence Model for Aerodynamic Flows”. La Recherche Aérospatiale, No. 1 (1994), pp. 5-21.

[10] F. R. Menter. "Two-Equation Eddy-Viscosity Turbulence Models for Engineering Applications". AIAA Journal, Vol. 32, No. 8 (1994), pp. 1598-1605.

[11] T. A. Harris. “NACA Technical Report No: 412, The 7 by 10 Foot Wind Tunnel of the National Advisory Committee for Aeronautics”. NACA. 1933.

[12] C. Ciray. *Akiskanlar Mekanigine Giris [Introduction to Fluid Mechanics]*. ODTU Yayincilik. 2013.

[13] L. Qiu and W. Song. “Efficient Decoupled Hydrodynamic and Aerodynamic Analysis of Amphibious Aircraft Water Takeoff Process”. Journal of Aircraft, Vol. 50, No. 5 (2013), pp. 1369-1379.